Bandwidth and Noise of Submillimeter Wave Cuprate Bicrystal Josephson Junction Detectors

Gennady A. Ovsyannikov, Igor V. Borisenko, Karen Y. Constantinian, Yulii V. Kislinski, Arsen A. Hakhoumian, Nubar G. Pogosyan, Tigran Zakaryan, Niels F. Pedersen, Jesper Mygind, Nikolaos Uzunoglu, and Evangelia Karagianni

***Abstract*—Detectors made from superconducting cuprate YBa_2Cu_3Ox bicrystal Josephson junctions (BJJs) on sapphire and $NdGaO_3$ substrates have been fabricated and characterized in the frequency band 200–900 GHz. Junctions on sapphire substrates had a normal state resistance $R_N \approx 15 - 60\ \Omega$, and $I_C R_N$ product up to 2.5 mV at $T = 4.2$ K. Junctions on $NdGaO_3$ substrates had lower $R_N = 1 - 5\ \Omega$ and $I_C R_N = 0.4$–0.9 mV at $T = 77$ K. Three types of detecting devices have been investigated in both the broadband and the frequency-selective detection modes. One type was patterned with log-periodic antenna, and two others with Pt-metal double-slot antenna designed for a central frequency $f = 300$ GHz and $f = 400$ GHz, respectively. Measurements at $f = 320$ GHz of the reception bandwidth Δf for a device with double-slot antenna gave a quality factor $Q = f/\Delta f \approx 10$. A low-noise cooled 1–2 GHz bandwidth amplifier enables a better sensitivity in the self-pumping frequency mixing mode, avoiding the 1/f noise. The dependence of the spectral density of noise on voltage was compared to the data for the Josephson emission linewidth obtained by the selective detector response method. Also discussed are measurements at 500 GHz of the NEP values carried out at different experimental conditions.**

***Index Terms*—High-temperature cuprate superconductors, Josephson junction, submillimeter wave devices.**

I. Introduction

DEVELOPMENTS of THz time-domain spectroscopy may lead to promising applications in biology, physics, micro-electronics, THz-wave imaging, etc. [1]. This, however, has been hampered by the lack of useable and efficient sensors. The high sensitivity and low power consumption of Josephson detectors make them attractive for applications at submm wave frequencies [2]. The weak coupling between two high-T_c cuprate grains with the crystallographic axis misoriented by an angle α has been used to realize bicrystal Josephson junctions (BJJs) [3]. The high values of R_N and the critical frequency $f_C = (2e/h)I_C R_N$ (I_C is the critical current), as well as the absence of hysteresis in the *I-V* curve even at $T = 4.2$ K, make the BJJs superior to low-T_C superconducting shunted tunnel junctions.

Here we present the results of fabrication and characterization of two types of cuprate Josephson junctions on sapphire and $NdGaO_3$ bicrystal substrates. The BJJs on sapphire substrates had high R_N values suitable for RF matching, but exhibit large $I_C R_N > 1$ mV at low temperatures, $T < 20$ K. Junctions on $NdGaO_3$ had $I_C R_N = 0.4$–0.9 mV at liquid nitrogen temperature $T = 77$ K, but smaller $R_N = 1 - 5\ \Omega$. The spectral characteristics of BJJ detectors, coupled with different submm wave antennas, have been studied both in the frequency-selective detection mode, as well as in the self-pumping mode using the low noise cooled amplifier.

II. Experimental

BJJs were fabricated either on in-plane tilted r-cut (1102) sapphire bicrystal substrates [4], or on novel basal plane tilted $NdGaO_3$ substrates [5]. The $YBa_2Cu_3O_x$ (YBCO) film was grown at 750–770°C by dc sputtering (in diode configuration) at high oxygen pressure (4 mbar). For sapphire substrates the CeO_2 epitaxial buffer layer was deposited by RF magnetron sputtering at 600–750°C under pressure 0.01 mbar in an Ar/O_2 mixture. The CeO_2 buffer layer prevents diffusion of Al atoms from the substrate into the YBCO film. The 5 μm wide and 10 μm long thin-film YBCO bridges crossing the bicrystal boundary were initially formed by RF plasma etching and chemical etching in a 0.5% Br_2 ethanol solution.

The submm wave BJJ detectors were integrated with log-periodic or double-slot antennas. Patterned YBCO strip lines of the double-slot antenna (20 μm width and 300–500 μm long) were covered with 200 nm thick metal Pt film which was fabricated by magnetron sputtering. Measurements were carried out in different experimental environments. For temperatures around $T = 20$ K we used a closed cycle cryosystem equipped with a Teflon window cryochamber. At higher temperatures around $T = 77$ K we used a nitrogen cryostat equipped with an optical 0.1 mm thick polyethylene film window. The backward wave oscillators (BWO) used as microwave signal sources were tunable in the bands 220–550 GHz and 800–900 GHz. The power was delivered to the sample via a set of Teflon lenses and an extended silicon hemispheric lens. The sapphire or $NdGaO_3$ chip was mounted on the flat side of the hemispheric

Manuscript received October 5, 2004. This work was supported in part by INTAS-2001-0809, INTAS-2001-0249, ISTC 2369, RFBR 04-02-6818, and PGSS 1344.2003.2.

G. A. Ovsyannikov, I. V. Borisenko, K. Y. Constantinian, and Y. V. Kislinski are with the Institute of Radio Engineering and Electronics Russian Academy of Sciences, Moscow 125009, Russia (e-mail: gena@hitech.cplire.ru).

A. A. Hakhoumian, N. G. Pogosyan, T. Zakaryan are with the Institute of Radio Physics and Electronics of National Academy of Armenia, Ashtarak-2, Armenia, (e-mail: arsen@irphe.am).

N. F. Pedersen is with the Technical University of Denmark, Department of Electric Power Engineering, Lyngby DK-2800, Denmark (e-mail: nfp@eltek.dtu.dk).

J. Mygind is with the Technical University of Denmark, Department of Physics, DK-2800 Lyngby, Denmark (e-mail: myg@fysik.dtu.dk).

N. Uzunoglu and E. Karagianni are with the National Technical University of Athens, Institute of Communication and Computer Sciences, Athens 157 73, Greece (e-mail: nnap@otenet.gr).

Digital Object Identifier 10.1109/TASC.2005.849902

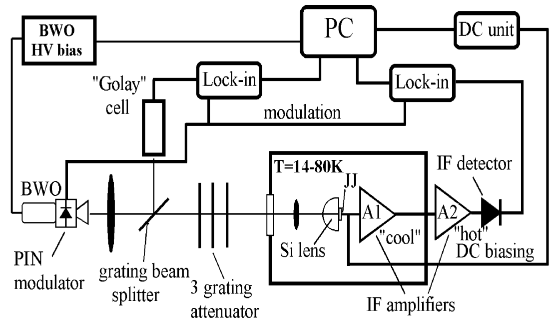

Fig. 1. Block diagram of set-up. The BWO is a submm wave source $f = 220$–550 GHz or 800–900 GHz. The PIN modulator is specially designed for the THz frequency range. The beam splitter is made from a metallic net. For simplicity the set of Teflon lenses is shown as one. The Golay cell is a submm wave detector. The Si hemispherical lens has diameter $\mathrm{d} = 12\ \mathrm{mm}$ and extension 3 mm. The JJ indicates the substrate with the BJJ and the integrated antenna.

lens. The 2 mm diameter radiation beam from the BWO was propagated in a 150 cm long quasioptical waveguide and then focused on the thin-film antenna with an average spot size of 0.1 mm. The diffraction divergence of the beam was 23 degrees at a wavelength of 0.75 mm.

Fig. 1 shows a simplified block diagram of the experimental set-up. This system was used also for simultaneous lock-in measurements of the amplitude of the detector response. Here the sweep rate was computer controlled. The BWO output signal is modulated by a chopper, or by a modified PIN-diode modulator mounted in a rectangular W-band waveguide. The PIN-diode modulator allows us to increase the modulation frequency F up to few kHz. In order to measure the spectral characteristics a fraction of the emitted power is splitted into a reference channel equipped with a Golay cell (optoacoustic detector). The reference channel is operated at a low modulation frequency $F = 32\ \mathrm{Hz}$, while the signal channel modulation could be tuned up to $F = 2$ kHz. The resulting amplitude-frequency characteristic (AFC) is the ratio between the Josephson junction detector response and the signal from the reference channel evaluated for incremented fixed frequencies. The junction dc bias voltage in the nonselective broadband detection mode was kept at $V = 200\ \mu\mathrm{V}$. In the frequency selective mode the voltage was continuously swept in order to plot the whole detector response function $\eta(V)$, which allows for estimation of the Josephson radiation linewidth. In the self-pumping mixing mode a cooled HEMT intermediate frequency amplifier (IFA) was connected directly to the BJJ to measure the down-converted output signal.

III. Amplitude-Frequency Characteristics

A. Detector Response

The *I-V* curves of the BJJs on both types of substrates were very similar to that of the resistively shunted junction (RSJ) model [6]. When subjected to a weak submm wave signal with fixed frequency f_e a symmetric odd-resonance shape of the selective detector response was registered at $V \approx hf_e/(2e)$. The broadband detector response was measured for $V \ll I_C R_N$, in particular at the bias voltage $V = 200\ \mu\mathrm{V}$. Fig. 2 shows the *I-V* curve and $\eta(V)$ plot, obtained for a BJJ at $T = 80$ K.

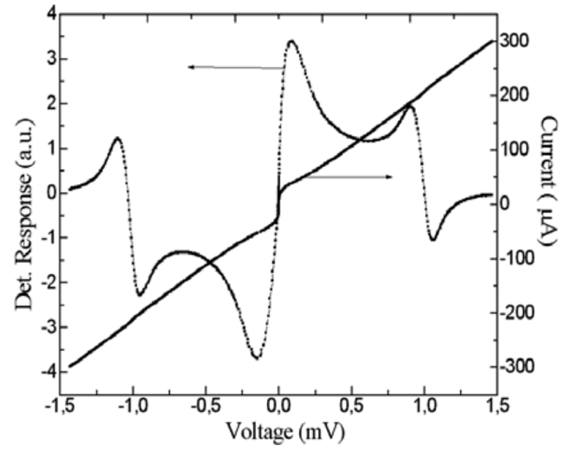

Fig. 2. Detector response of bicrystal Josephson junction on $\mathrm{NdGaO_3}$ substrate for $\mathrm{T} = 80\ \mathrm{K}$. An external 500 GHz radiation was applied. The response has two distinct features: first is the wideband response at low voltages and second is the frequency selective response at voltage $V = hf_e/(2e)$.

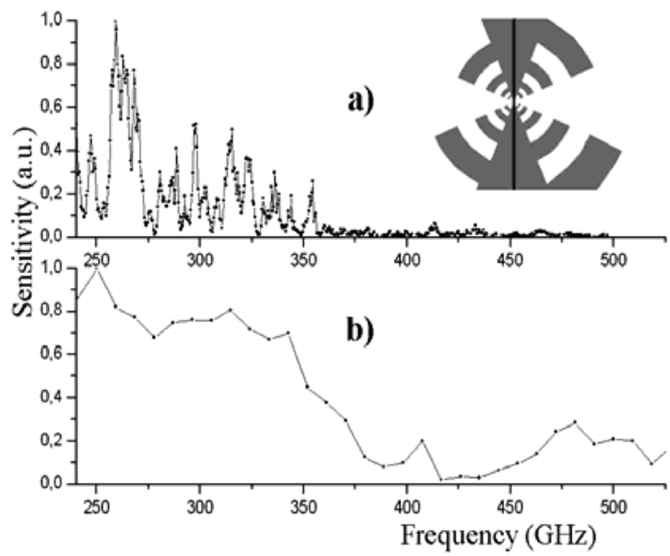

Fig. 3. Amplitude-frequency characteristics for a log-periodic antenna with a BJJ on sapphire at $T = 20\ \mathrm{K}$. (a) a metal (platinum) antenna was used, (b) all HTSC sample, evaluated by use of Fourier Transform Spectrometer.

The linewidth of the Josephson oscillation was measured in the current-source biasing regime. For the particular case shown in Fig. 2 the linewidth is 2.8 times larger than predicted by the RSJ model [9].

B. Log-Periodic Antenna

Fig. 3(a) and Fig. 4 show the spectral characteristics measured with the set-up depicted in Fig. 1. The response of the log-periodic antenna-coupled BJJ is reduced for frequencies $f_e > 350\ \mathrm{GHz}$ (Fig. 3). Fig. 3(b) shows the AFC, obtained separately by use of a Fourier Transform Spectrometer (FTS) [7] with the BJJ biased at $V = 1.15\ \mathrm{mV}$. Fig. 3(b) also shows a downward slope in the $\eta(V)$ dependence on V. The rapid variations seen in Fig. 3(a) may be due to frequency dependent variations of radiation pattern from the swept BWO, while the smoother dependence shown in Fig. 3(b) was obtained using a Hg-tube noise signal source.

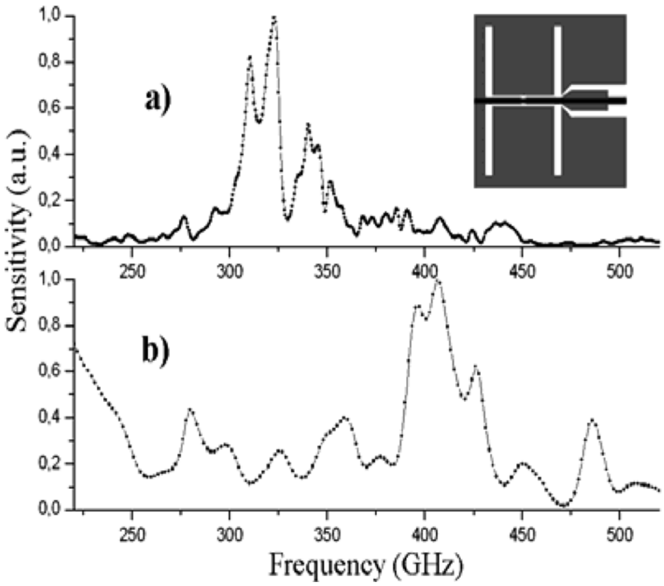

Fig. 4. Amplitude-frequency characteristics for double-slot line antenna designed for 300 GHz (a) and 400 GHz (b). Resonance peaks with quality factor $Q = 6$ are clearly observed.

C. Double-Slot Line Antenna

The inset in Fig. 4(a) shows a sample designed [8] for 300 GHz with double-slot antenna. The AFC had about 20 dB response ratio P_{MAX}/P_{MIN} with a sharp peak around $f_e = 320$ GHz. The corresponding bandwidth is 50 GHz, giving a quality factor $Q = 6$. At the various frequencies the applied power was adjusted so that the minimum detected power P_{MIN} was roughly of the same order allowing for minor variations in different samples and experimental conditions. The applied power was kept sufficiently small to ensure quadratic signal detection, and throughout the measurement the maximum detected power P_{MAX} was much smaller than the saturation power. However, we did not measure the dynamic range for the BJJ, but we believe that it is much larger than 20 dB.

In an other sample with double-slot line antenna, designed for 400 GHz (Fig. 4(b)), we observed several peaks at frequencies within the band $f_e = 300$–450 GHz. This may be explained by the influence on the antenna pattern of the asymmetrical band-stop filters, which are inserted in order to improve the impedance matching of the BJJ to the IF output circuit. If so a new design is required with improved impedance matching at both the input and the output frequency bands.

IV. Noise Parameters

A. Noise of Bicrystal Josephson Junctions

Previous studies [9] showed that thermal fluctuation in BJJs dominates at high temperatures $T \sim 77$ K and above. However, for low noise applications detectors should be cooled down to $T = 4.2$ K, where the excess shot noise is caused by the multiple Andreev reflection process [10].

Fig. 5 shows the *I-V* curve and noise power $P_N(V)$ measured in two different frequency bands for a BJJ on sapphire substrate.

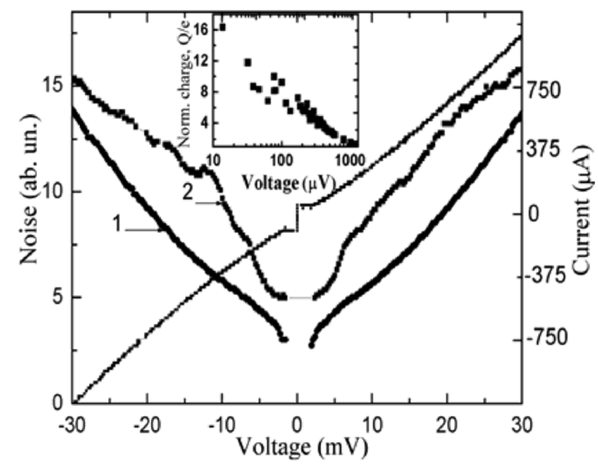

Fig. 5. The *I-V* curve and noise power $P_N(V)$ in the 1–2 GHz frequency band (curve 1), and the 3–300 kHz band (curve 2) for a BJJ on sapphire substrate at $T = 4.2$ K. Inset: noise/current ratio in terms of effective transferred charge $q(V)$ for bias voltages $V < 1$ mV.

The inset shows the voltage dependence of the effective transferred charge $q(V)$, demonstrating noticeable noise rise for decreasing bias voltage $V < 1$ mV at $T = 4.2$ K. A broadening (by a factor 3–10) of the Josephson oscillation linewidth for both BJJ types on sapphire and tilted $NdGaO_3$ substrates was found also at intermediate temperatures $T = 20$–45 K in our measurements of the selective detector response functions at different frequencies between 350–500 GHz.

B. Radiometric Measurements

The noise equivalent power, NEP, giving the sensitivity of broadband detecting devices was measured in the modulator radiometric regime.

In order to estimate the minimal detecting power we use a submm wave attenuator which was calibrated using a standard Golay cell with $\mathrm{NEP} = 0.4\ \mathrm{nW/Hz^{1/2}}$ up to a wavelength of 2 mm. As a simple test of the NEP of the BJJ we compare the minimal detecting power P_{MIN} for the BJJ and the Golay cell, using a calibrated double-grating variable attenuator with an aperture much larger than the beam size. A variable diaphragm reducing the beam aperture was used to further reduce the BWO input power. An alternative power calibration method is based on the well known dependence of the Shapiro step height on RF current amplitude. At a relatively high signal level we measured the Shapiro step $I_1 = 6\mu$A at $T = 80$ K. The $V_C = I_C R_N$ product was 130 μV and hence the normalized frequency at 500 GHz is $\omega = f_e/f_C = 8$ (Fig. 6(a)).

First we used the Bessel-function dependence of the Shapiro step we can calculate the RF current amplitude $I_{RF} = 1/2\omega I_1 = 23\ \mu$A and the applied power $P = 1/2 I_{RF}^2 R_N = 1.3$ nW. Then for increasing attenuation by switching the external power on and off we plotted the noise trace. At the lowest signal/noise ratio (Fig. 6(b)) we estimated the NEP to $6 \cdot 10^{-13}\ \mathrm{W/Hz^{1/2}}$ and the voltage sensitivity $\eta = \Delta V/\Delta P = 2 \cdot 10^4$ V/W. The theoretical prediction [6] gives $\mathrm{NEP} = 20 \cdot \omega^2 \cdot k_B T \cdot f_C^{1/2}$ equal to $3 \cdot 10^{-13}\ \mathrm{W/Hz^{1/2}}$ with our parameters only two times lower than the obtained experimental value.

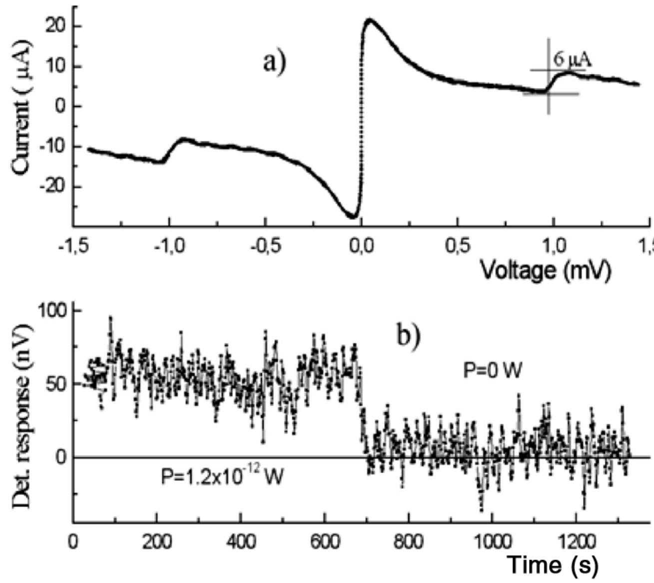

Fig. 6. Calibration of absorbed power and radiometric measurements at $f = 500$ GHz, $T = 80$ K a)—Josephson part of reduced *IV*-curve $(I(V) - I \cdot (R_N)$ with Shapiro steps which allow us to estimate the power absorbed by the junction at high signal levels. b)—noise trace at low signal-to-noise ratio for known absorbed power. The NEP is estimated to $6 \cdot 10^{-13} \mathrm{W/Hz}^{1/2}$.

V. Conclusion

Thin film bicrystal YBCO Josephson junctions (BJJs) on in-plane tilted sapphire and on basal-plane tilted $NdGaO_3$ substrates were fabricated and characterized by their noise factor and submm wave signal detecting properties. Our BJJs had an $I_C R_N$ product up to 2,5 mV at 4.2 K on sapphire substrates, and up to 1 mV at $T = 77$ K on $NdGaO_3$ substrates. Submm wave detector response was studied in wide range of temperatures $T = 14$–81 K and amplitude-frequency characteristics have been obtained for the devices integrated in different antennas. Due to a noticeable reduction of the detector response at $T/T_C > 0.7$ the $NdGaO_3$ substrate samples with higher $I_C R_N$ product at $T = 77$ K are preferable. Generally the operating temperature should be around 20 K. Neglecting the coupling loss we have measured a Noise Equivalent Power, $\mathrm{NEP} = 6 \cdot 10^{-13}\ \mathrm{W/Hz}^{1/2}$ at $T = 81$ K, $f = 500$ GHz for a bicrystal Josephson detector built on basal-plane tilted $NdGaO_3$ substrate coupled with a log-periodic antenna.

Acknowledgment

The authors would like to thank I. M. Kotelyanski, A. V. Shadrin, and V. K. Kornev for fruitful discussions and help in the experiment.

References

[1] X.-C. Zhang, “Terahertz wave imaging: horizons and hurdles,” *Phys. Med. Biol.*, vol. 47, pp. 3667–3677, 2002.

[2] Y. V. Divin, O. Y. Volkov, M. Liatti, V. V. Shirotov, V. V. Psavlovskii, U. Poppe, P. M. Shadrin, and K. Urban, “Hilbert spectroscopy from gigahertz to terahertz frequencies by high-T_C Josephson junctions,” *Physica C*, vol. 372–376, pp. 416–419, 2002.

[3] H. Hilgenkamp and J. Mannhart, “Grain boundaries in high- Tc superconductors,” *Rev. Mod. Phys.*, vol. 74, pp. 485–549, 2002.

[4] A. D. Mashtakov, K. Y. Constantinian, G. A. Ovsyannikov, and E. A. Stepantsov, “YBCO Josephson junctions on a bicrystal sapphire substrate for devices in the millimeter and submillimeter wavelength rages,” *Technical Physics Letters*, vol. 25, pp. 249–252, 1999.

[5] I. V. Borisenko, I. M. Kotelyanski, A. V. Shadrin, P. V. Komissinski, and G. A. Ovsyannikov, “Josephson dynamics of [100] tilted Y-B-C-O bicrystal junctions on $Nd\text{-}Ga\text{-}O_3$,” in *ASC’04*.

[6] K. K. Likharev, *Dynamics of Josephson Junctions and Circuits*. New York: Gordon and Breach, 1986.

[7] K. Y. Constantinian, G. A. Ovsyannikov, I. V. Borisenko, and P. Yagoubov, “Observation of a voltage-tunable sub-mm wave response from a YBCO Josephson device, operating in self-pumping mode,” *Supercond. Sci. Technology*, vol. 14, pp. 1005–1008, 2001.

[8] P. Focardi, A. Neto, and W. R. McGrath, “Coplanar-waveguide-based terahertz hot-electron-bolometer mixer-improved embedding circuit description,” *IEEE Trans. Microw. Theory Tech.*, vol. 50, pp. 2374–2383, 2002.

[9] Y. V. Kislinskii, K. Y. Constantinian, I. V. Borisenko, G. A. Ovsyannikov, and P. Yagoubov, “Submm wave signal detection by bicrystal YBCO Josephson junctions at liquid nitrogen temperatures,” *Physica C*, vol. 372–376, pp. 436–439, 2002.

[10] K. Y. Constantinian, G. A. Ovsyannikov, I. V. Borisenko, J. Mygind, and N. F. Pedersen, “Shot noise in YBCO bicrystal Josephson junctions,” *IEEE Trans. Appl. Superconduct.*, vol. 13, pp. 610–613, 2003.